Effect of Reaction Rate on Morphological Change of Reactive Blends

Hyun Kyoung Jeon and Jin Kon Kim*

Department of Chemical Engineering and Polymer Research Institute, Electric and Computer Engineering Divisions, Pohang University of Science and Technology, Pohang, Kyungbuk, 790-784, Korea

Received May 16, 2000

ABSTRACT: The effect of reaction rate on the morphology of reactive blends has been studied using 75/25 (wt/wt) monocarboxylated polystyrene [PS-mCOOH]/poly(methyl methacrylate) [PMMA] with poly(methyl methacrylate-*ran*-glycidyl methacrylate) [PMMA-GMA] as an in-situ compatibilizer, by varying the amount of PMMA-GMA in the blend, the molar concentration of GMA, $C_{GMA,0}$ in PMMA-GMA at fixed molecular weight, and the molecular weight of PMMA-GMA at fixed $C_{GMA,0}$. For the blends with PMMA−GMA having lower $C_{GMA,0}$, there exists a critical amount of PMMA−GMA above which a sharp decrease in the surface area average domain size (D_s) occurs. This amount was shifted to a smaller value with increasing $C_{GMA,0}$ in PMMA-GMA. We demonstrated that the interfacial graft reaction between PS-mCOOH and PMMA-GMA at 220 °C was described by the simple second-order reaction kinetics, i.e., mean field reaction kinetics. From the morphological evolution, it is found that the morphological change by an external flow from a pellet size to D_s with less than 1 μm occurred within a very short time of ∼30 s. After this transition, coalescence is the main mechanism for determining the final morphology obtained at a mixing time of 20 min. Finally, a master curve is obtained when D_s is plotted against $C_{GMA,0}$, implying again that the concept of mean field reaction kinetics adequately applies to the blends employed in this study.

Introduction

The morphological development of polymer blends has long been investigated since it significantly affects the final mechanical properties. However, most polymer blends are immiscible thermodynamically and exhibit coarse morphology that results in poor mechanical properties. Therefore, a compatibilization technique using physical or reactive compatibilizers has been widely employed to control desirable morphology. The morphology of a compatibilized polymer blend is fine and stable for further processings.

It is found that the major reduction of the dispersed phase size during a melt blending occurs at an initial stage of less than 1−2 min.[1−6] For reactive blends, reaction kinetics should be considered. If the reaction rate is much faster than the morphological development rate, the size of the dispersed phase will be very small and similar to the size of microphase-separated block copolymer.[7−10] However, despite its importance, there has been little research on the effect of reaction rate on the morphology of a reactive blend.[7,11,12] According to the theories on reaction kinetics at polymer interfaces, the reaction rate constant k is expressed differently depending on the chain dynamics and the reactivity.[13−17] For sufficiently large reactivity the reaction kinetics is diffusion-controlled, but mean field kinetics is applied to the small reactivity for both the Rouse and reptation regimes.

In this study we investigated the effect of the reaction rate on the morphology of a reactive blend consisting of monocarboxylated polystyrene (PS-mCOOH) and poly(methyl methacrylate) (PMMA) with poly(methyl methacrylate-*ran*-glycidyl methacrylate) (PMMA-GMA) as an in-situ compatibilizer. The reaction between the carboxylic acid in PS-mCOOH and the epoxy groups in PMMA−GMA occurs easily at higher temperatures,[12,18−22] giving the in-situ graft copolymers of PMMA-*g*-PS. The reaction rate of this blend was systemically varied by changing the amount of PMMA-GMA in the blend, the molar concentration of GMA, $C_{GMA,0}$ in PMMA-GMA at fixed molecular weight, and the molecular weight of PMMA−GMA at fixed $C_{GMA,0}$. In this paper, we report the highlights of our findings.

* To whom all correspondence should be addressed. E-mail: jkkim@postech.ac.kr.

Experimental Section

The molecular characteristics of polymers employed in this study are listed in Table 1. PS-mCOOH and PMMA were purchased from Aldrich Chemical Co. and Polysciences, Inc., respectively. All PMMA-GMAs used in this study were prepared by free radical polymerization. The GMA concentration in PMMA−GMA was easily controlled by using different mole ratios of GMA monomer to MMA monomer added initially into a reactor since the reactivity ratios of GMA and MMA are 0.71 and 0.52, respectively.[23] The molar concentration of GMA in PMMA-GMA was determined by a 500 MHz proton nuclear magnetic resonance spectroscope (^{1}H NMR; DRX 500, Bruker). All polymers were dried for 24 h at 70 °C under vacuum before melt blending. The 75/25 (wt/wt) PS-mCOOH/PMMA blends with various amounts of PMMA−GMA as an in-situ compatibilizer were prepared using a MiniMax molder at 220 °C. Total weight of each blend was 0.5 g, and the maximum shear rate was 20 s^{-1}. The mixing was carried out for 20 min under nitrogen atmosphere, even though the morphology of most blends was fixed within 10 min mixing. However, for the blends with low GMA concentrations, such as the blend with 20 wt % PMMA-GMA2H, the morphology continued to change after 10 min mixing. The morphology of the blend was observed using by a field emission scanning electron microscope (FE-SEM; S-4200, Hitachi). The blend was cryogenically fractured. To enhance the contrast of the dispersed phase of PMMA, the fractured surface was further etched by using acetic acid, which is a solvent for PMMA but a nonsolvent for PS. Then the surface area average diameter D_s of the dispersed phase was determined by the Quantimet 570 image analyzer (Cambridge Instrument). About 200−300 particles are employed to calculate D_s. The cross-sectional area (A_i) of each particle on

10.1021/ma000842i CCC: $19.00
Published on Web 10/11/2000

Table 1. Molecular Characteristics of Polymers Used in This Study

polymer	M_n	M_p	M_w/M_n	mol % of GMA in PMMA-GMA	no. of functional groups (f) per chain[a]	η^* (Pa·s) at $\omega = 20$ rad/s and 220 °C
PS-mCOOH	89 000	167 000	1.50		1	640
PMMA	45 000	71 000	1.79	0	0	960
PMMA-GMA0.3H	53 000	87 000	1.79	0.3	2.6	1610
PMMA-GMA2H	53 000	63 000	1.55	2.0	12.5	1420
PMMA-GMA0.7L	32 700	35 000	1.46	0.7	2.4	*b*
PMMA-GMA2L	28 800	27 000	1.58	2.0	5.4	*b*
PMMA-GMA8L	28 600	30 000	1.60	8.3	24.1	220

[a] Values based on M_p. [b] Not measured due to the limited amounts available.

the micrograph was measured and then converted to the diameter (D_i) of circle having the same cross-sectional area.

$$D_i = 2(A_i/\pi)^{1/2} \quad (1)$$

$$D_s = \sum_i D_i^3 / \sum_i D_i^2 \quad (2)$$

The (PMMA + unreacted PMMA−GMA) phase and PMMA-*g*-PS formed in-situ during melt blending were separated from the unreacted PS-mCOOH in each blend by using the solvent mixture of 80/20 v/v cyclohexane/toluene. It was confirmed that this mixed solvent was a nonsolvent for PMMA but a good solvent for the unreacted PS-mCOOH. Gel permeation chromatography (GPC; Waters 600E, Millipore) with UV detector and ^{1}H NMR were employed to measure the molecular weight and the weight fraction of PMMA-*g*-PS formed in-situ in the blend, respectively.[24,25] However, since the hydrodynamic volume for homopolymers (or PMMA-*block*-PS) might be different from that for PMMA-*g*-PS, the molecular weight of PMMA-*g*-PS determined by GPC with PS calibration curve might be different from the absolute molecular weight obtained with a laser light scattering, even though it was reported that the difference in measured molecular weights by GPC with PS calibration curve between the six-arm star PS and linear PS with the same degrees of polymerization is less than 20%.[26,27] To test this argument, we prepared the 75/25 (wt/wt) PS-mCOOH/PMMA-GMA blend, and PS-mCOOH in the blend was first removed as described above. Then, we removed the unreacted PMMA-GMA in the mixture of PMMA-*g*-PS and PMMA-GMA by dissolving it out using acetic acid for 4 days at 60 °C. Then PMMA-*g*-PS itself was separated from the solution by using an ultracentrifuge at 8000 rpm. The absolute molecular weight of PMMA-*g*-PS was determined by GPC equipped with MALLS (multiangle laser light scattering) (GPC-MALLS) at the Department of Chemistry in POSTECH, Korea, with a measured value of dn/dc. The detectors in GPC-MALLS employed were a UV detector (UV 100, Spectra series), an RI detector (Optilab 903, Wyatt Technology), and a MALLS detector (Mini-Dawn, Wyatt Technology). The PMMA-*g*-PS solution in THF (0.2 wt % in solid) was injected at a rate of 0.8 cm^3/min. When GPC-MALLS is employed, the absolute values of the number-average and weight-average molecular weights (M_n and M_w) and the molecular weight at peak (M_p) in GPC-MALLS are simultaneously determined.

Using GPC-MALLS with the measured value of dn/dc = 0.155 cm^3/g, the M_p and M_w of PMMA-*g*-PS itself prepared by 75/25 (wt/wt) PS-mCOOH and PMMA-GMA8L were determined to be 215 000 and 255 000.[25] Since the M_p and M_w calculated from GPC only with PS standards were 209 000 and 251 000, the difference between the two methods (GPC with PS calibration and GPC-MALLS) is within experimental error (±10%). We also found that the M_p and M_w of PMMA-*g*-PS itself prepared by 75/25 (wt/wt) PS-mCOOH and PMMA-GMA2H were determined to be 230 000 and 430 000 when GPC-MALLS with the measured value of dn/dc = 0.144 cm^3/g was used.[25] Since the M_p and M_w calculated from GPC only with PS standards was 227 000 and 424 000, the difference between the two methods is also within experimental error. Therefore, we conclude that the molecular weights of PMMA-*g*-PS obtained from GPC only with PS calibration were quite reasonable. This little difference between two methods, namely the negligible effect of hydrodynamic effect between PMMA-*g*-PS and PS (or PMMA and PS-*block*-PMMA)), might be due to fact that (i) the retention volume of PMMA is very similar to that of PS at the same molecular weight (maximum difference is less than 20% at a given retention volume) and (ii) the number of graft chains of PS-mCOOH in PMMA-*g*-PS was found to be small (1−2);[25] thus, the chain conformation of PMMA-*g*-PS obtained in this study is not much different from PMMA-*block*-PS.

Results

SEM images of 75/25 (wt/wt) PS-mCOOH/(PMMA + PMMA-GMA8L) with various amounts of PMMA-GMA8L are shown in Figure 1, and those with various amounts of PMMA-GMA0.7L are shown in Figure 2. The weight fraction of PMMA-GMAxL was on the basis of total PMMA phase. It is seen in Figure 1 that, with increasing amount of PMMA-GMA8L, D_s decreases rapidly up to 10 wt % of PMMA-GMA8L and then decreases very slowly and gradually. Also, the adhesion between the matrix and the dispersed phase becomes stronger since fractured surfaces are rougher. This phenomenon given in Figures 1 and 2 is often found for a reactive polymer blend where the dispersed phase size in a reactive blend decreases rapidly at a small amount (say less than about 10 wt %) of an in-situ compatibilizer and then levels off.[28−30] However, as shown in Figure 2, D_s for the blend with PMMA-GMA0.7L does not decrease up to 50 wt %; then it decreases suddenly to the final dispersed domain size. Of course, D_s of a blend with 100 wt % of PMMA-GMA0.7L was 0.77 μm, which is larger than that (0.23 μm) of another with 100 wt % of PMMA-GMA8L. This is due to the difference in the number of epoxy groups per a PMMA-GMA chain (f); for instance, f of PMMA-GMA8L is ∼10 times higher than that of the former. The change in D_s with amount of L-series of PMMA-GMA for 75/25 PS-mCOOH/PMMA with three different PMMA-GMAxLs is given in Figure 3. Of course, the variation of D_s with the amount of PMMA-GMA2L falls between PMMA-GMA8L and PMMA-GMA0.7L blend systems. Interestingly, D_s for blends with 100 wt % of L-series of PMMA-GMA is not proportionally decreased to f, even though the higher f, the smaller D_s.

The variation of D_s with the amount of H-series of PMMA-GMA is given in Figure 4. The largest decrease in D_s was observed at ∼50 wt % for PMMA-GMA2H, while that was observed at ∼75 wt % for PMMA-GMA0.3H. This behavior is similar to the results given in Figure 3. The reduced domain size (D_r),[19,31] defined by the ratio of the domain size (D_s) of each blend composition with 100% of PMMA-GMA to that ($D_{s,0}$) of respective blend composition without PMMA-GMA, for PMMA-GMA2H was 0.17, which is smaller than that (0.38) for PMMA-GMA0.3H. Thus, the efficiency of the domain reduction ($1 - D_r$) for PMMA-GMA2H is just

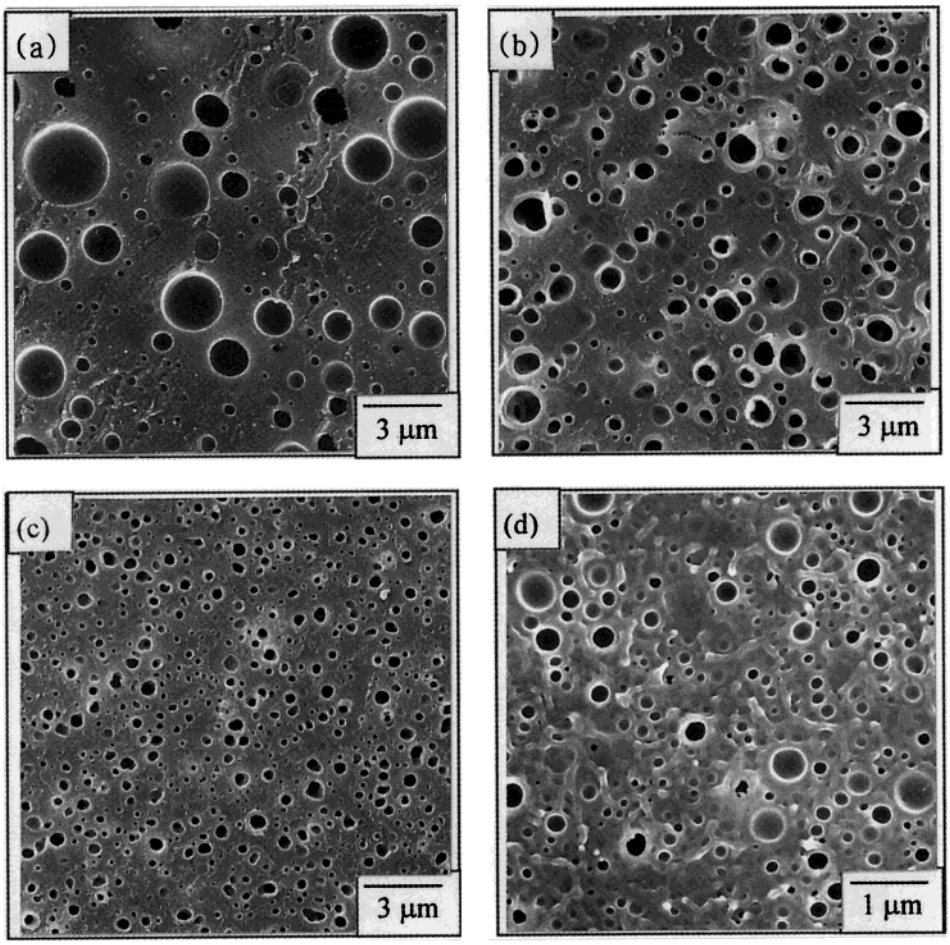

Figure 1. SEM images of 75/25 (wt/wt) PS-mCOOH/PMMA with various amounts of PMMA-GMA8L based on total PMMA phase: (a) 0 wt %, (b) 10 wt %, (c) 50 wt %, and (d) 100 wt %.

1.3 times larger than that for PMMA-GMA0.3H, even though f in the former is 6.25 times larger than that in the latter. Also, if we lower the molecular weight of PMMA-GMA at the constant molar concentration of GMA (compare PMMA-GMA2L with PMMA-GMA2H), the amount of PMMA-GMA2L at which the largest decrease in D_s is observed is smaller than that of PMMA-GMA2H. Therefore, these results led us to conclude that the dispersed domain size was easily stabilized for in-situ compatiblizer having a large total number of chains per unit volume but smaller f compared with another having smaller total number of chains per unit volume but larger f. Furthermore, the increase in f at the same molecular weight lowers the critical amount of PMMA-GMA above which the largest decrease in D_s is observed.

The decrease in D_s is related to the copolymer weight fraction $w_{copolymer}$(blend) of PMMA-*g*-PS formed in-situ during melt blending. To determine $w_{copolymer}$(blend), the phase consisting of PMMA and unreacted PMMA-GMA as well as PMMA-*g*-PS was separated from unreacted PS-mCOOH in the blends using the solvent extraction method.[24,25] The $w_{copolymer}$(blend) was calculated from the weight fraction of PS in the extracted PMMA phase w_{PS}(extract) measured directly using ^{1}H NMR.

$$w_{copolymer}(\text{blend}) = \frac{w_{PS}(\text{extract}) w_{PMMA} M_{copolymer}}{n M_{PS-mCOOH}} \quad (3)$$

where w_{PMMA} is the weight fraction of the dispersed PMMA phase in the blend (0.25 in this study), $M_{copolymer}$ and $M_{PS-mCOOH}$ are the molecular weights of PMMA-*g*-PS and PS-mCOOH, respectively, and n refers to the average number of PS-mCOOH chains grafted on a PMMA-GMA chain. As reported elsewhere,[25] n depends on the choice of which molecular weights for PMMA-*g*-PS, PS-mCOOH, and PMMA−GMAs are used, because all neat homopolymers and in-situ formed grafted copolymers are polydisperse. Namely, n obtained on the basis of the weight-average molecular weight (n_w) is different from than that obtained on the basis of the peak molecular weight (n_p). For instance, the n_p and n_w of PMMA-*g*-PS itself prepared by 75/25 (wt/wt) PS-mCOOH and PMMA-GMA8L were 1.1 and 1.5, while those of PMMA-*g*-PS itself prepared by 75/25 (wt/wt) PS-mCOOH and PMMA-GMA2H were 1.0 and 2.6. But n_p was used throughout this study because of the straightforward determination of the peak molecular weights in GPC chromatogram. Also, $M_{copolymer}$ corresponding to M_p, which was determined by GPC with PS standards, was employed. Furthermore, we assume that $M_{copolymer}$ in the blends with 20 and 50 wt % of PMMA-GMA2H is the same as that in the blend with 100 wt % of PMMA-GMA2H. Similarly, $M_{copolymer}$ in the blends with 50 wt % of PMMA-GMA0.3H is assumed to be the same as that in blend with 100 wt % of PMMA-GMA0.3H. This is because the copolymer weight fraction formed in-situ in those blend, especially the blends with 20 and 50 wt % of PMMA-GMA2H and PMMA-GMA0.3H, respectively, were very low; thus, it was not easy to measure the molecular weight of PMMA-*g*-PS

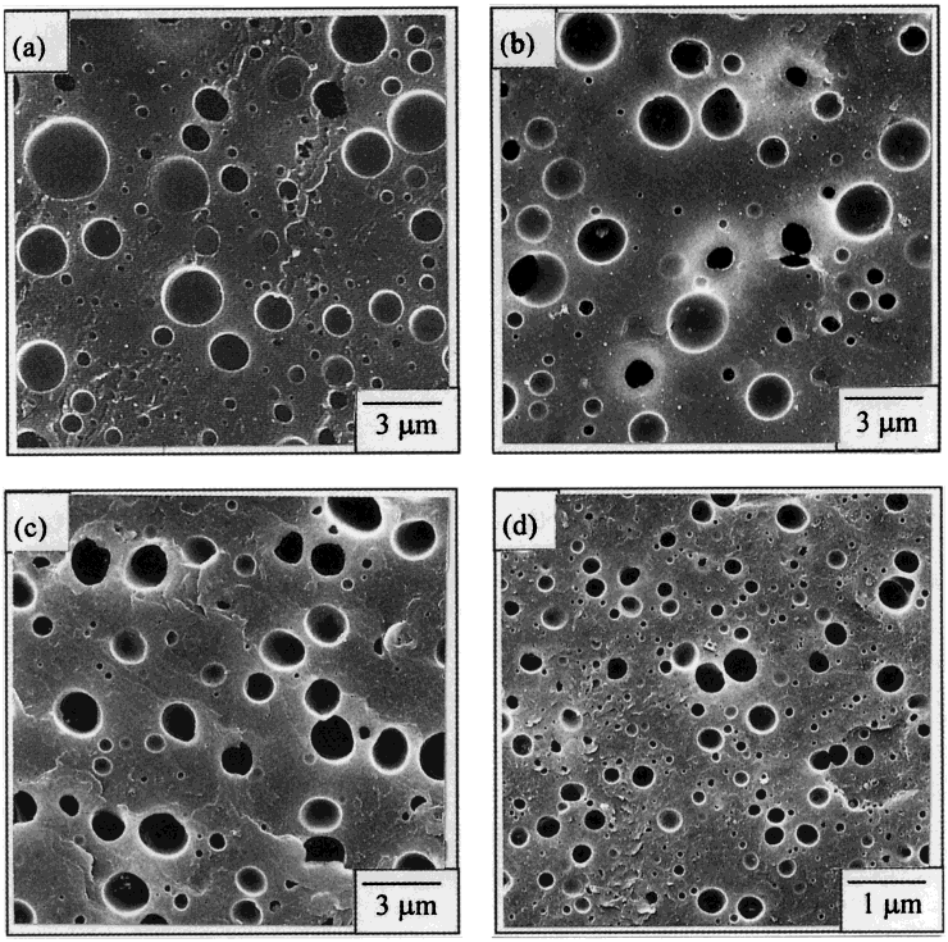

Figure 2. SEM images of 75/25 (wt/wt) PS-mCOOH/PMMA with various amounts of PMMA-GMA0.7L based on total PMMA phase: (a) 0 wt %, (b) 20 wt %, (c) 50 wt %, and (d) 100 wt %.

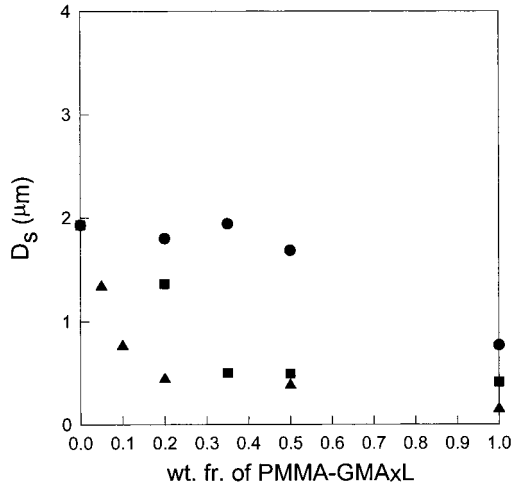

Figure 3. Plots of D_s versus the amount of L-series of PMMA-GMA based on total PMMA phase for 75/25 (wt/wt) PS-mCOOH/PMMA: (●) PMMA-GMA0.7L, (■) PMMA-GMA2L, and (▲) PMMA-GMA8L.

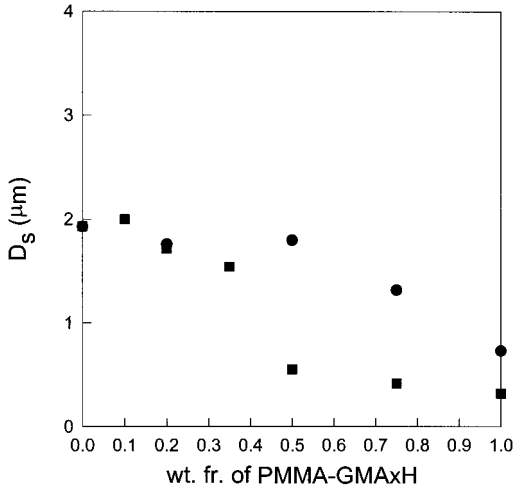

Figure 4. Plots of D_s versus the amount of H-series of PMMA-GMA based on total PMMA phase for 75/25 (wt/wt) PS-mCOOH/PMMA: (●) PMMA-GMA0.3H and (■) PMMA-GMA2H.

by GPC even if it was possible to determine the w_{PS}(extract) by NMR. With these values and eq 3, $w_{copolymer}$(blend) for each blend is determined and given in Table 2. Interestingly, for blends with 20 wt % of PMMA-GMA2H or 50 wt % of PMMA-GMA0.3H where D_s did not decrease and had almost the same size for the blends without PMMA-GMA, $w_{copolymer}$(blend) was indeed very low (say ~0.3 wt %). In Table 2 is also shown the interfacial area density Σ calculated by

$$\Sigma = \frac{w_{copolymer}(\text{blend}) N_{av} \rho_{blend} D}{6 M_{copolymer} \phi_d} = \frac{w_{PS}(\text{extract}) w_{PMMA} N_{av} \rho_{blend} D}{6 n M_{PS-mCOOH} \phi_d} \quad (4)$$

Here, N_{av} is Avogadro's number, ρ_{blend} is the density of

Table 2. Weight Fraction and Interfacial Areal Density of PMMA-*g*-PS Formed in Situ in 75/25 wt/wt PS-mCOOH/(PMMA + PMMA-GMAH) Blends

PMMA-GMA	PMMA-GMA2H			PMMA-GMA0.3H	
wt % of PMMA-GMA	20	50	100	50	100
D_s (μm)	1.72	0.55	0.32	1.80	0.73
w_{PS}(extract) (wt %)	1.13	5.44	9.50	0.93	3.90
$w_{copolymer}$(blend) (wt %)	0.38	1.85	3.2	0.32	1.4
Σ (chains/nm^2)[a]	0.012	0.019	0.019	0.011	0.018

[a] Calculated by using M_p of PMMA-*g*-PS formed in-situ in the blends.[25]

the blend, D is the diameter of the dispersed domain, and ϕ_d is the volume fraction of the dispersed phase. ρ_{blend} is calculated by using a mixing rule, $\rho_{blend} = w_{PS}\rho_{PS} + w_{PMMA}\rho_{PMMA}$, where w_i is the weight fraction of blend component i and ρ_{PS} and ρ_{PMMA} at 220 °C are 0.96[32] and 1.06 g/cm^3,[33] respectively.

It is seen in Table 2 that Σ is almost constant ($\sim$0.02 chain/nm^2) regardless of the initially added amounts of the in-situ compatibilizer except two blends with 20 wt % PMMA-GMA2H and 50 wt % PMMA-GMA0.3H. We previously reported that Σ was constant ($\sim$0.1 chain/nm^2) for PBT/PS blend with an in-situ compatibilizer of PS-GMA regardless of the initially added amounts of PS-GMA.[22] The small Σ might be due to the smaller interaction parameter χ (0.027) of PS and PMMA at 220 °C.[35] Thus, near the interface of the blend with low χ, the in-situ formed graft copolymers need not stretch much. This implies that most of the reactions are confined to the reactants that are already located near the interface and that the interface can be stabilized by a relatively low Σ. However, Schulze et al.[36] recently reported that the molecular weight (M) of an end-functional polymer profoundly affected the value of Σ of a block (or graft) copolymer formed in-situ in a reactive blend; for instance, the larger M, the smaller Σ. Thus, the smaller Σ of graft copolymers prepared by PS-mCOOH/PMMA-GMA blend compared with that prepared by PBT/PS-GMA blend[22] might be due to the fact that the $M_{PS-mCOOH}$ is 2−5 times larger than $M_{PMMA-GMAs}$ in this blend (see Table 1), whereas the M_{PBT} is about half of that M_{PS-GMA} in PBT/PS-GMA blend.[22]

These results suggest the coalescence of the dispersed phase to be greatly suppressed even at a small value of Σ ($\sim$0.02 chain/nm^2). Thus, we considered that even if a small dispersed domain size would be achieved for blends with 20 wt % of PMMA-GMA2H or 50 wt % of PMMA-GMA0.3H at short mixing time less than 1 min by the flow, the amount of $w_{copolymer}$(blend) would be very small due to relatively slow reaction rate. In this situation, the in-situ formed PMMA-*g*-PS chains do not cover fully the entire dispersed domain size. Thus, with increasing mixing time, owing to dynamic coalescence, the smaller dispersed domain would increase up to the final domain size whose Σ is $\sim$0.02 chain/nm^2. However, when the mole fraction of GMA increased, enough amount of PMMA-*g*-PS was formed; thus, this graft copolymers can cover the entire smaller dispersed domain size. In this situation, dynamic coalescence was greatly suppressed, resulting in the very small final domain size. According to Macosko et al., the value of $\sim$0.02 chain/nm^2 for Σ was sufficient to prevent a dynamic coalescence.[37]

Discussion

The results given in Figures 3 and 4 and Table 2 suggest that the changes in the reaction rate due to different amounts of GMA in PMMA-GMA and/or molecular weight of PMMA-GMA affect profoundly the final dispersed domain size. Especially, as long as the concentration of GMA in a blend is lower, with increasing amount of PMMA-GMA, D_s does not decrease up to a critical amount; then a sharp decrease in D_s is observed. It is known that D_s can be estimated by the relative magnitude of the reaction rate ($dC_{copolymer}/dt$) to the interfacial area generation rate (dA_{int}/dt).[7] Here $C_{copolymer}$ is the concentration of graft copolymer in the blend. If $\Sigma(dA_{int}/dt)$ is faster than $dC_{copolymer}/dt$ (namely slow reaction), the newly generated area by the external flow does not have enough amounts of the in-situ formed copolymers. Thus, in this situation the final D_s would be larger. There are two major reasons for a larger D_s: First, due to the small concentration of in-situ formed copolymers, it is difficult to reduce the interfacial tension and stabilize the interface, implying that the breakup of the large dispersed phase to the smaller one is unfavorable. The other is that the flow, such as shearing and/or extensional flow, creates a very large interfacial area; thus, the ratio of the interfacial area by the flow to the initial interfacial area, A/A_0, becomes infinite within a very short time (say less than 1−2 min). Of course, the interfacial reaction occurs simultaneously with variations of interfacial area. However, if $dC_{copolymer}/dt$ at that time is too slow for the in-situ formed graft copolymers to prohibit the coalescence of dispersed phase, the interfacial area continues to decrease to the time that the minimum amounts of the graft copolymers to prevent further coalescence are formed at the interface. While if $\Sigma(dA_{int}/dt) \leq dC_{copolymer}/dt$ (or faster reaction), enough graft copolymers are formed within short time (say less than 1 min). Thus, the coalescence is significantly suppressed, implying that a finer dispersed phase does not change with further mixing time.

To test these two possibilities, we carried out morphological evolutions with time for 75/25 (wt/wt) PS-mCOOH/PMMA with two different amounts of PMMA-GMA2H (20 wt % vs 50 wt % PMMA-GMA2H). Interestingly enough, as shown in Figures 5 and 6, $D_s \sim 0.5\ \mu$m at a mixing time of 30 s for both blends is very similar. It is noted that, in measuring D_s that is used to calculate Σ (see eq 4), the nonspherical dispersed domains as shown in Figures 5 and 6 are treated as spheres with the same area (see eq 1). Since the nonspherical hole density was $\sim$10% of the observed image by FESEM, any possible error in determining D_s using eqs 1 and 2 would be small.

The measured D_s is 1 order of magnitude larger than the prediction ($D \sim 0.06\ \mu$m) by the Taylor theory.[38,39]

$$D = \frac{4\Gamma(\eta_r + 1)}{\dot{\gamma}\eta_m\left(\frac{19}{4}\eta_r + 4\right)} \tag{5}$$

Here, Γ of 0.79 mN/m between PS and PMMA was used.[40] η_r ($=\eta_d/\eta_m$) and η_m for PS-mCOOH at $\dot{\gamma}$ of 20 s^{-1} and 220 °C were 1.5 and 640.6 Pa s, respectively. The larger experimental value of D compared with the prediction is attributed to the coalescence effect during the initial mixing[41] and viscoelastic effect of polymers.

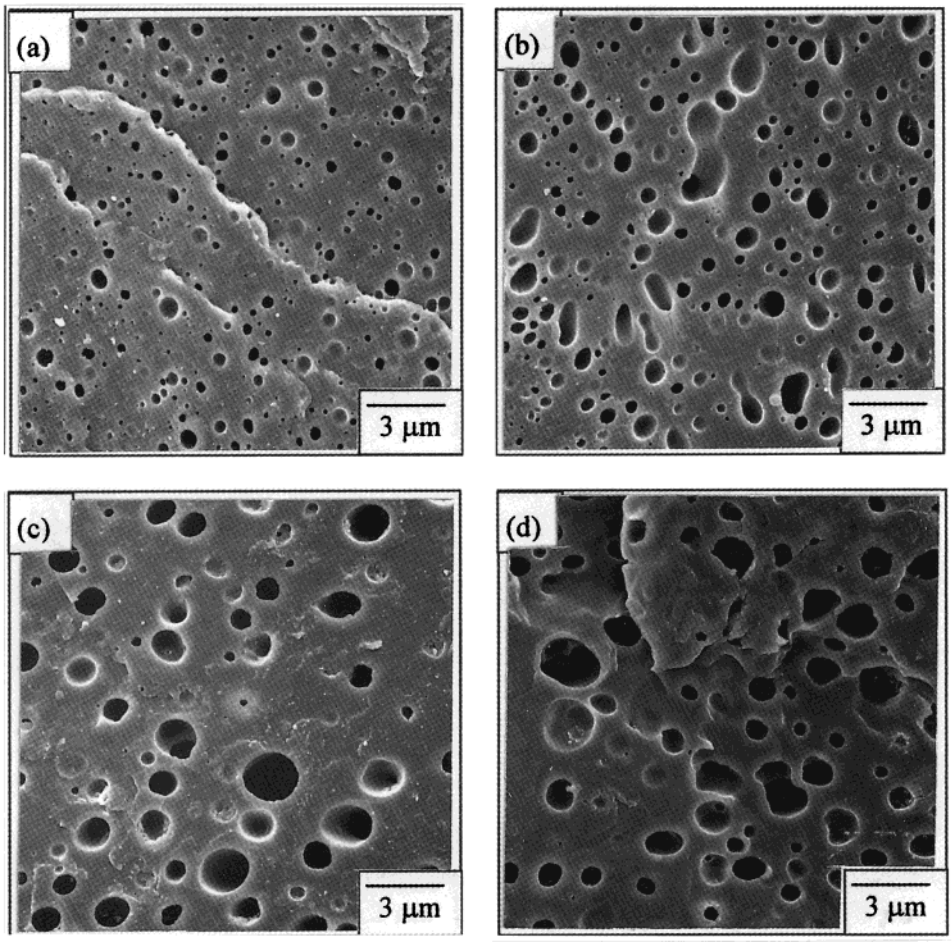

Figure 5. SEM images of the morphology evolution with mixing time for 75/25 (wt/wt) PS-mCOOH/PMMA with 20 wt % of PMMA-GMA2H based on total PMMA phase: (a) 30 s, (b) 60 s, (c) 360 s, and (d) 600 s.

In this situation, when we the employed Wu equation,[42]

$$D = 4\eta_r^{0.84}\Gamma/\dot{\gamma}\eta_m \tag{6}$$

the predicted D is 0.35 μm, which is close to the experimental value.

However, with increasing mixing time, D_s for a blend with 20 wt % of PMMA-GMA2H increased steadily due to the shear-induced coalescence resulting in a larger domain size similar to the blend without PMMA-GMA. On the other hand, D_s for the other blend with 50 wt % of PMMA-GMA2H was not changed anymore, resulting in a smaller domain size. These results led us to conclude that a large D_s at the mixing time of 20 min for 20 wt % of PMMA-GMA2H is mainly attributed to a shear (or flow)-induced coalescence owing to insufficient amounts of graft copolymers to prevent the coalescence. But a smaller interfacial tension reduction, owing to smaller amounts of graft copolymer needed for breaking the larger domain into the smaller domain by the external flow, is not a main source to have a larger D, even though this effect is not completely excluded. Thus, the reduction of Γ from the reduction in disperse domain size with amount of an in-situ compatibilizer should be estimated very carefully, unless the volume fraction of the dispersed domain is extremely small (say less than 0.1%) in which a coalescence is significantly excluded. On the basis of the above results, we conclude that the final dispersed domain size prepared in a molten state is significantly affected by the reaction rate, i.e., reaction kinetics which in turn depends on the reaction pair, and the amount of functional group as well as molecular weight and temperature.

Kramer[43] derived the expressions describing the grafting kinetics of end functional polymers. The grafting density of end functional polymers, Σ, with time can be obtained by

$$\int_0^{\xi} d\xi \exp\left(\frac{\mu^*(\xi)}{k_B T}\right) = \frac{t}{\tau_i} \tag{7}$$

$$\xi = \frac{z^*}{R_g} = \frac{N\Sigma}{\rho_0 R_g} \tag{8}$$

$$\frac{\mu^*(\xi)}{k_B T} = \frac{3}{4}\xi + 1.1 \ln\left(\frac{R_g}{\delta}\right) \tag{9}$$

where $\mu^*(\xi)$ is the chemical potential of a polymer chain in the brush, z^* is the interfacial excess of the grafted chains in the brush, N is the degree of polymerization of end functional polymers, ρ_0 is the segment density of end functional polymers $[1/\{v_{sp}[M]_0\}$ in which v_{sp} is the specific volume and $[M]_0$ is the monomeric molecular weight of the end-functionalized polymer, R_g is the radius of gyration, δ is the interfacial thickness, and τ_i is the characteristic time expressed as

$$\tau_D = \frac{R_g \delta}{D} = \frac{M_0^2 N^{5/2} a \delta}{6^{1/2} D_0} \quad \text{for the diffusion-controlled} \tag{10}$$

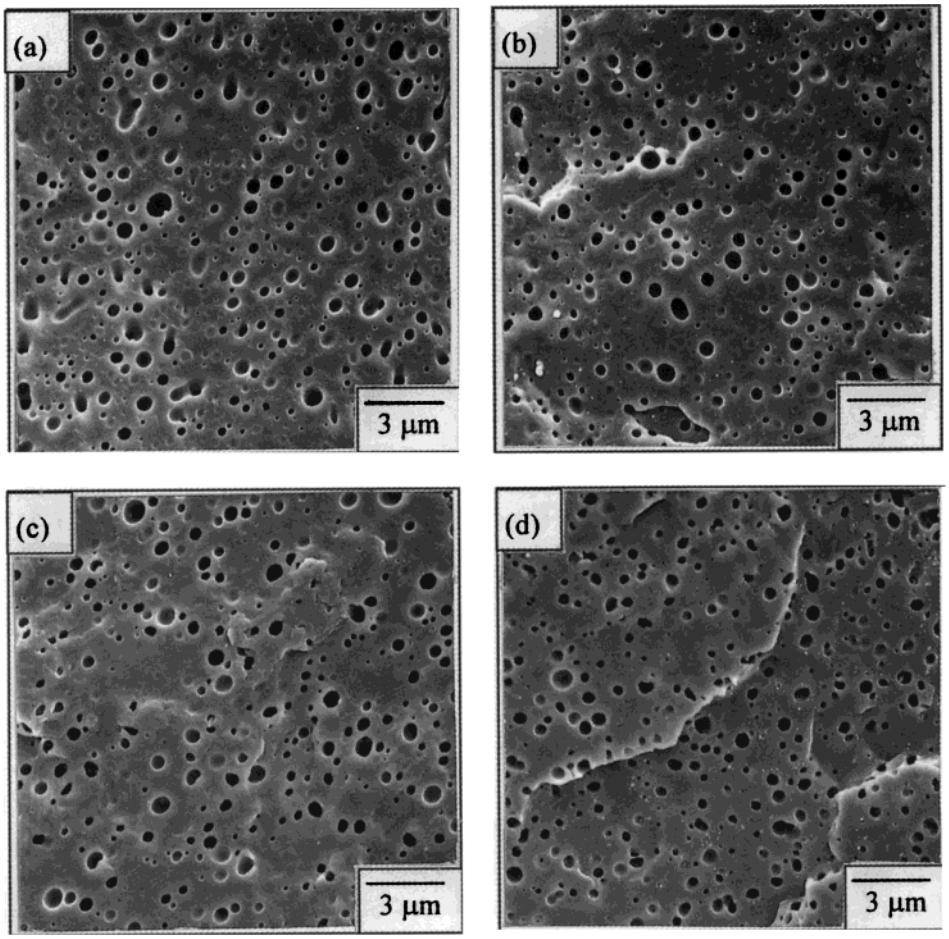

Figure 6. SEM images of the morphology evolution with mixing time for 75/25 (wt/wt) PS-mCOOH/PMMA with 50 wt % of PMMA-GMA2H based on total PMMA phase: (a) 30 s, (b) 60 s, (c) 180 s, and (d) 360 s.

$$\tau_R = \frac{R_g}{kC_B\delta} = \frac{N^{1/2}a}{6^{1/2}kC_B\delta} \quad \text{for the reaction-controlled} \tag{11}$$

where a is the statistical segment length, D is the self-diffusion coefficient ($=D_0/M^2$), M_0 is the molecular weight of a monomer, k is the reaction rate constant, and C_B is the concentration of B reactive groups in the interfacial layer which react with A reactive groups of end functional polymers in the interface region. He assumed that C_B does not change by the interfacial reaction due to $C_B \gg (\rho_0/N)$ for A reactive group. For PS-mCOOH used in this study, N is 1606, M_0 is 104 g/mol, a is 0.67 nm, δ is 5 nm,[44] and D is calculated to be 5.6×10^{-12} cm^2/s at 220 °C.[45] Also, k between PS-mCOOH and PMMA-GMA8L at 220 °C was estimated to be 0.3 kg mol^{-1} s^{-1} [50] from the results given in Guégan et al.[12] The largest value of $C_{GMA,0}$ (C_B), which is the case of PMMA-GMA8L in this study, is 0.803 mol/kg. From eqs 10 and 11, τ_D and τ_R are 0.098 and 9.10 s, respectively. Therefore, it can be concluded that the reaction in all PS-mCOOH/(PMMA + PMMA-GMA) blends prepared in this study is reaction-controlled. Very recently, Schulze et al.[36] concluded that the reaction between amino-terminal deuterated PS and anhydride-terminal PMMA is also reaction-controlled.

We found that the prediction of Σ with time using eqs 7−9 and 11 was quite different from the experimental value. For instance, the predicted Σ at 1200 s was 0.06−0.09 chains/nm^2 depending on $C_{GMA,0}$, which is 3−5 times larger than the experimental value (∼0.02 chains/nm^2 as shown in Table 2). The difference between the estimated and the experimental values of Σ stems from the assumption of the infinite concentration of one reactive groups in Kramer's theory.[43] According to this assumption, interfacial reaction continues until the concentration of carboxylic acid in the interfacial region vanishes, and then the fresh PS-mCOOH chains near the interface or even far from the interface can approach the interface through an energy barrier [$\exp(-\mu^*(\xi)/k_BT)$ of graft copolymer layers. This fresh PS-mCOOH can react with excess GMA located in the interface since $C_{GMA,0} > C_{COOH,0}$. Thus, even if $d\Sigma/dt$ decreases with reaction time, Σ increases steadily, which implied that the prediction of Σ can be overestimated.

Therefore, although eqs 7−9 are useful to describe the interfacial reaction kinetics in the dry brush limit, it is unlikely for this concept to be applied to the reactive blends of PS-mCOOH/(PMMA + PMMA-GMA) prepared by a mixer in the molten state, especially the blends with the concentration ratio of (C_{GMA}/C_{COOH}) ≤ $O(1)$ because the change of C_{GMA} due to the interfacial reaction cannot be neglected and the grafted PS-mCOOH chain does not stretch. Because of the above-mentioned reasons, we proposed a simple second-order reaction to describe the interfacial reaction in the blends of PS-mCOOH/(PMMA + PMMA-GMA). O'Shaughnessy and co-workers[17] proposed that simple second-order reaction kinetics should apply until the interface saturates with copolymer, and a transition to diffusion-controlled reaction kinetics will not be observed for reactive blend containing amine/anhydride and epoxy/

carboxylic acid pairs. Furthermore, Jiao[51] modified the Kramer model[43] (namely, eqs 7−9 and 11) of a reactive polymer system where the concentration of one component is rather small with a reaction-controlled limit. They argue that a chemical potentail barrier $\mu^*(\xi)/k_BT$ of graft copolymer layers would not be significant unless for the large ξ or Σ ($\xi > \xi_m \sim 0.8$).[36,51] For the blends employed in this study, Σ was ~0.02 nm^2/chains ($\xi \sim 0.4$); thus, the choice of a simple second-order reaction kinetics for our blend might be reasonable. Once the simple second-order reaction kinetics is employed, we have

$$\frac{dC_{copolymer}}{dt} = kC_{COOH}C_{GMA} \tag{12}$$

C_{COOH} and C_{GMA} are the concentrations of carboxylic acid and epoxy groups in mol/kg at the interface at time t, respectively. C_{COOH} and C_{GMA} at $t = 0$ are equal to the concentrations in the bulk, $C_{COOH,0} = (\rho_0/N_{PS-mCOOH})$, and $C_{GMA,0} = (\rho_0\phi f/N_{PMMA-GMA})$ where ϕ is the volume fraction of PMMA-GMA based on total PMMA phase. C_{COOH} at time t is $(C_{COOH,0} - nC_{copolymer})$ because n COOH groups (thus n PS-mCOOH chains) diminish for the formation of one copolymer chain. But C_{GMA} at time t is $(C_{GMA,0} - fC_{copolymer})$. This is attributed to the fact that once one copolymer with n grafted chains is formed, the rest of the GMAs in PMMA-GMA belonging to that copolymer chain become inactive. Using these results, eq 12 is integrated over t.

$$C_{copolymer}(t) = \frac{C_{COOH,0}C_{GMA,0}\{\exp[kt(fC_{COOH,0} - nC_{GMA,0})] - 1\}}{fC_{COOH,0}\exp[kt(fC_{COOH,0} - nC_{GMA,0})] - nC_{GMA,0}} \tag{13}$$

$$\Sigma(t) = C_{copolymer}(t)\delta \tag{14}$$

Figure 7 shows the variations of $\Sigma(t)$ with time up to $t = 1200$ s calculated by eqs 13 and 14 for PS-mCOOH/(PMMA + PMMA-GMAH) blends. Also shown in Figure 7 are experimental results (symbols) at 1200 s. From eq 13, $C_{copolymer}$ at a steady state (or very large values of t) becomes $C_{COOH,0}/n$ for $nC_{GMA,0} > fC_{COOH,0}$, while it becomes $C_{GMA,0}/f$ for $nC_{GMA,0} < fC_{COOH,0}$. Thus, the estimated Σ is shown to be very dependent on the relative magnitude of $C_{GMA,0}$ compared with $fC_{COOH,0}/n$. Here, we consider the case of $n = 1$ on the basis of n_p.[25] Except for two blends with 20 wt % of PMMA-GMA2H and 50 wt % of PMMA-GMA0.3H, all other blends have the relationship of $C_{GMA,0} > fC_{COOH,0}$. Thus, the $C_{copolymer}$ at larger times for these blends approach $C_{COOH,0}$, which is independent of the amount of $C_{GMA,0}$. But for a blend with 20 wt % of PMMA-GMA2H, $C_{GMA,0}/f$ is 3.17×10^{-3} mol/kg, which is lower than $C_{COOH,0}$ of 5.99×10^{-3} mol/kg. Also, for a blend with 50 wt % of PMMA-GMA0.3H, $C_{GMA,0}/f$ is 5.75×10^{-3} mol/kg, which is slightly smaller than $C_{COOH,0}$. In those two blends, the estimated Σ's for the two blends are affected largely by the $C_{GMA,0}$ and f. It is seen in Figure 7a that for a blend with 50 wt % of PMMA-GMA2H the experimentally measured Σ's (shown by symbol ■) at various reaction times are in good agreement with predictions given in curve 4. Furthermore, the experimentally measured Σ's at 1200 s for all blends employed in this study are also consistent with the estimated ones by the simple second-order reaction rate equation. This implies

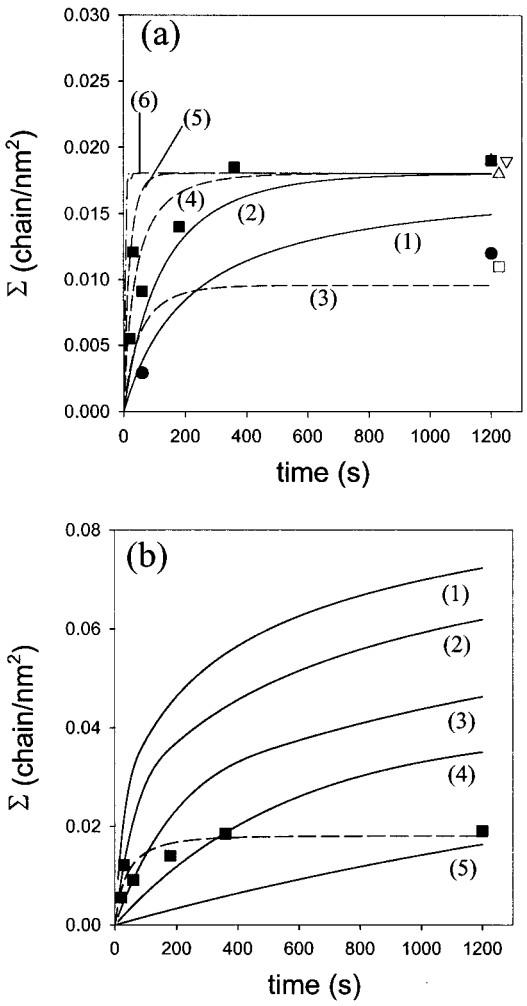

Figure 7. Upper panel (a): Interfacial area density (Σ) with time for the graft copolymers in-situ formed in the blends of PS-mCOOH/(PMMA + PMMA-GMA), estimated by the mean field reaction rate equation (eq 13 and 14): (1) 50 wt %, (2) 100 wt % of PMMA-GMA0.3H; (3) 20 wt %, (4) 50 wt %, (5) 100 wt % of PMMA-GMA2H, and (6) 100 wt % of PMMA-GMA8L. The experimental results at blend time of 20 min are given by symbols: (□) 50% of PMMA-GMA0.3H, (△) 100% of PMMA-GMA0.3H, (●) 20% of PMMA-GMA2H, (■) 50% of PMMA-GMA2H, (▲) 100% of PMMA-GMA2H, and (▽) 100% of PMMA-GMA8L. The measured values of Σ's at five different blends times of 20, 30, 60, 180, and 360 s for 50% of PMMA-GMA2H are shown as symbol (■). Lower Panel (b): Plot of Σ versus time for the graft copolymers in-situ formed in the blends with 50% of PMMA-GMA2H, estimated by the eqs 15a and 15b using five different k (kg mol^{-1} s^{-1}); (1) 0.3; (2) 0.15; (3) 0.05; (4) 0.02; and (5) 0.005. The symbol (■) represents the measured values of Σ. Dotted curve is the same as curve (4) in the upper panel.

that most of graft copolymers are formed only by the reaction between PMMA-GMA and PS-mCOOH located at the interface without further influx of reactant from the bulk.

It should be pointed out that a good agreement of Σ between the prediction and the experimental data, as shown in curve 4 of Figure 7a, might not necessarily guarantee the validity of simple second-order kinetics for reactive polymer blends. This is because of uncertainty in determining Σ and k. Although forward recoil spectrometry (FRES) gives an accurate Σ, this method could not be employed for a reactive blend prepared by a melt mixing. We consider that the error in the determination of Σ from eq 4 becomes smaller once the

measurement of n (or $M_{copolymer}$) becomes accurate. But, as described previously, n changes with which molecular weight of PMMA-*g*-PS is chosen. We found that n_p for all blends was ~1, while n_w was 2−3 depending upon the blend composition and system. Thus, the values of Σ obtained by using n_w become half or one-third of those reported in Table 2. However, even in this situation, because the prediction of Σ using eqs 13 and 14 was also decreased due to increased value of n, we found that the predicted values were also consistent with the measured ones even if n_w was used. These results led us to conclude that the simple second-order reaction kinetics is adequately applied to PMMA-GMA/PS-mCOOH blend because of a rather small value of Σ (or $\xi \sim 0.4 < \xi_m$ (=0.8−1.0)). Finally, we compared experimentally determined Σ with predictions made by Jiao[51] (also see ref 36) for $C_{GMA,0} > fC_{COOH,0}$ which was given by

$$\frac{d\xi}{dt} = k[C_{GMA}]_0\left(\frac{\delta}{R_{G,PS-mCOOH}}\right)^{2.1}\left(1 - \frac{\xi}{\xi_m} + \frac{\xi}{\xi_m}\exp\left(-\frac{3}{4}\xi_m^2\right)\right) \quad \text{for } \xi < \xi_m \quad (15a)$$

$$\frac{d\xi}{dt} = k[C_{GMA}]_0\left(\frac{\delta}{R_{G,PS-mCOOH}}\right)^{2.1}\exp\left(-\frac{3}{4}\xi^2\right) \quad \text{for } \xi \geq \xi_m \quad (15b)$$

The prediction of Σ with $\xi_m = 0.8$ [36] for the blend with 50% of PMMA-GMA2H is given in Figure 7b. It is noted that even though five different reaction constants of k (0.3, 0.15, 0.05, 0.02, and 0.005 kg mol^{-1} s^{-1}) were employed, the agreement between the predicted Σ and measured ones was poor. Namely, when predicted Σ matches with measured one at earlier times by adjusting k having 0.02−0.05 kg mol^{-1} s^{-1}, the prediction at later times becomes much larger than measured one. Also, when predicted Σ matches with measured one at later times by adjusting k having 0.005 kg mol^{-1} s^{-1}, the prediction at earlier times becomes much smaller than measured one. Of course, these k are 1−2 orders of magnitude smaller than the reported value (0.3 kg mol^{-1} s^{-1}), which was used in Figure 7a. Although Schulze et al.[36] reported that the value of k decreased with increasing molecular weight (M) of an end-functional polymer, the high M of PS-mCOOH compared with that of PMMA-GMAs (thus smaller k) was not a main source in the discrepancy. Rather, we consider that eqs 15a and 15b might be applicable to a reactive polymer blend without shearing such as the situation in ref 36, whereas eq 13 might be valid for a reactive polymer blend prepared by a melt mixer. It is seen in Figure 7 that Σ determined experimentally for the blend with 50 wt % of PMMA-GMA2H quickly reaches a steady value within 3−5 min, whereas the prediction does not reach a steady even at t = 20 min. These results led us to consider that the reaction under shearing from a melt mixing is quite a bit faster than that without shearing, which was also described in ref 36.

According to results given in Figures 5 and 6, interfacial area generation by flow was almost finished in less than 30 s for both blends with 20 and 50 wt % of PMMA-GMA2H. However, in the case of the blend with 20 wt % of PMMA-GMA2H, the dispersed domains continue growing up to the time at which the interface is covered by the minimum amount of graft copolymers needed to prohibit the coalescence. From Figure 5, this critical time is about 360 s, consistent qualitatively with the estimated time (~200 s) as shown in Figure 7. Therefore, we can consider that Σ of ~0.01 chain/nm^2 is sufficient to prevent the coalescence in the PS-mCOOH/(PMMA + PMMA-GMA) blends because the measured Σ of the blends with 20 wt % of PMMA-GMA2H is ~0.01 chain/nm^2. Meanwhile, judged by Figure 6, in the blend with 50 wt % of PMMA-GMA2H, 30 s is sufficient time for the interfacial reaction to make enough PMMA-*g*-PS to prevent further coalescence. From the curve 4 in Figure 7, the critical time at which Σ becomes 0.01 chain/nm^2 was predicted to be ~30 s, and further increase to Σ above 0.02 chain/nm^2 is because the remains of reactive groups at the interface continue to react until one reactive group of the two is consumed completely and to cover the interface fully. Therefore, we can conclude that the simple second-order reaction rate equation is adequately applied to estimate the reaction rate, i.e., the copolymer formation rate, for reactive polymer blends prepared by a melt blending. Especially the reaction in the blends with a relatively low χ such as PMMA/PS blend is well expressed by the second-order reaction rate equation since the effect of chain stretching would not be important.

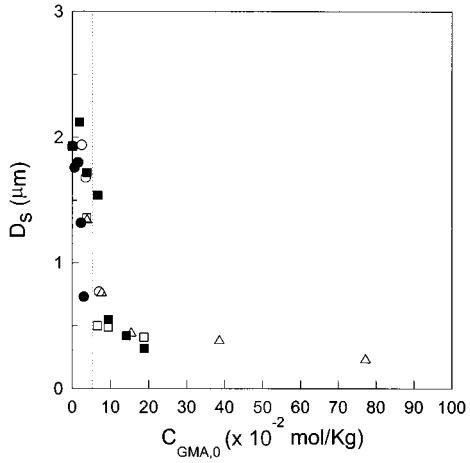

Figure 8. D_s versus $C_{GMA,0}$ for all 75/25 (wt/wt) PS-mCOOH/(PMMA + PMMA-GMA) blends prepared in this study: (○) PMMA-GMA0.7L, (□) PMMA-GMA2L, (△) PMMA-GMA8L; (●) PMMA-GMA0.3H, and (■) PMMA-GMA2H.

According to eq 14, at constant t and $C_{COOH,0}$, the copolymer concentration, $C_{copolymer}$(blend) depends on $C_{GMA,0}$ itself. Since $C_{copolymer}$(blend) is inversely proportional to D_s as shown in eq 4, plots of D_s of the blends versus $C_{GMA,0}$ give a single master curve, which is indeed shown in Figure 8 for all blends employed in this study. Also, it can be seen that the critical $C_{crit,GMA,0}$ at which the sharp decrease in D_s occurs is ~0.05 mol/kg (marked by vertical dotted line in Figure 8). When the concentration of GMA is larger than this value, the morphology in the blends of PS-mCOOH and PMMA-GMA at 220 °C is finer due to sufficiently suppressing coalescence by the flow. Since this critical concentration would be shifted depending on the reaction rate constant, k, it would be interesting to investigate whether this value for amine/maleic anhydride (MA) polymer pairs where one polymer has only one functional unit at the chain end (say polyamide 6) is indeed decreased. Although comprehensive studies to investigate the critical concentration of MA ($C_{crit,MA,0}$) to suppress the coalescence of the disperse phase (thus very finer structure) are not available in the literature, we notice

one report[52] that the disperse domain size of poly(styrene-*co*-maleic anhydride) (SMA) in the blend of 80/20 (wt/wt) polyamide 6/SMA with 0.075 wt % of MA in SMA was 1 order of magnitude smaller than that in the blend of 80/20 (wt/wt) polyamide 6/PS. Also, for the MA contents in SMA larger than ~0.22 wt %, the dispersed domain size does not change irrespective of the initially added content of MA. Therefore, in this blend, $C_{crit,MA,0}$ would be less than ~0.02 mol/kg (or even as small as 0.0075 mol/kg). Furthermore, Koriyama et al.[53] reported that when MA content in poly(sulfone-*g*-maleic anhydride) (PSU-*g*-MA) is larger than 0.2 wt % (which is the minimum value in their study), the interfacial thickness between PSU-*g*-MA and amorphous nylon with one functional group at the chain end is larger enough, implying that a coalescence is effectively suppressed. Of course, one considers that $C_{crit,MA,0}$ would be less than 0.02 mol/kg. This is why polymers with MA functional group are frequently employed in the industry for in-situ compatibilizer for blends containing polyamide.[54]

Conclusions

In this study we have shown that the reaction rate, depending upon the amount of PMMA-GMA in the blend, the molar concentration of GMA in PMMA-GMA at fixed molecular weight, and the molecular weight of PMMA-GMA at fixed molar concentration of GMA, affects significantly the morphology of 75/25 (wt/wt) PS-mCOOH/(PMMA + PMMA-GMA) blends.

For the blends with PMMA-GMA having lower molar concentrations of GMA, there exists a critical amount of PMMA-GMA above which a sharp decrease in the surface area average domain size (D_s) occurs. This amount was shifted to a smaller value as the molar concentration of GMA in PMMA-GMA was increased. However, the interfacial areal density Σ of PMMA-*g*-PS formed in-situ was nearly constant as ~0.02 chains/nm^2 regardless of the amounts of PMMA-GMA in the blend, the molar concentrations of GMA in PMMA-GMA, and the molecular weights of PMMA-GMA. These results were explained by using the concept of interfacial reaction kinetics and morphological evolution.

We demonstrated that the interfacial graft reaction between PS-mCOOH and PMMA-GMA at 220 °C was not diffusion-controlled but reaction-controlled. Also, the simple second-order reaction kinetics, i.e., the mean-field reaction kinetics, given by eqs 12−14 is well applied to the above polymer blends prepared by melt blending. From the morphological evolution, it is found that the morphological change by an external flow from a pellet size to D_s with less than 1 μm occurred within a very short time of ~30 s. After this transition, the coalescence is the main mechanism for determining the final morphology obtained at the mixing time of 20 min. Therefore, if the reaction rate is too slow, thus the amount of in-situ formed PMMA-*g*-PS is insufficient to prevent coalescence, coarse morphology is obtained. Finally, the master curve is obtained when D_s is plotted against the concentration of GMA ($C_{GMA,0}$) in the blend initially added, implying again that the concept of mean field reaction kinetics applies adequately to the blends employed in this study. To stabilize the morphology in the blends of PS-mCOOH and PMMA-GMA at 220 °C, the critical $C_{GMA,0}$ would be ~ 0.05 mol/kg.

Acknowledgment. We acknowledge Prof. T. Chang, Mrs. H. T. Oh, and M. S. Lee at POSTECH for kindly measuring the absolute molecular weights of PMMA-*g*-PS using by GPC-MALLS. Profs. C. W. Macosko in U. of Minnesota and K. Char in Seoul National U. critically read this manuscript. This work was supported by the Korea Research Foundation (1998-001-e01369) and BK 21 program.

References and Notes

(1) Plochocki, A. P.; Dagli, S. S.; Andrews, R. D. *Polym. Eng. Sci.* **1990**, *30*, 741.
(2) Favis, B. D. *J. Appl. Polym. Sci.* **1990**, *39*, 285.
(3) Scott, C. E.; Macosko, C. W. *Polym. Bull.* **1991**, *26*, 341.
(4) Scott, C. E.; Macosko, C. W. *Polymer* **1994**, *35*, 5422.
(5) Sundararaj, U.; Macosko, C. W. *Polym. Eng. Sci.* **1996**, *37*, 1769.
(6) Sundararaj, U.; Dori, Y.; Macosko, C. W. *Polymer* **1995**, *36*, 1957.
(7) Orr, C. A.; Adedeji, A.; Hirao, A.; Bates, F. S.; Macosko, C. W. *Macromolecules* **1997**, *30*, 1243.
(8) Lyu, S.-P.; Cernohous, J. J.; Bates, F. S.; Macosko, C. W. *Macromolecules* **1999**, *32*, 106.
(9) Ibuki, J.; Charoensirisomboon, P.; Chiba, T.; Ougizawa, T.; Inoue, T.; Weber, M.; Koch, E. *Polymer* **1999**, *40*, 647.
(10) Jiao, J.; Kramer, E. J.; de Vos, S.; Möller, M.; Koning, C. *Polym. Commun.* **1999**, *40*, 3585.
(11) Scott, C.; Macosko, C. *J. Polym. Sci., Polym. Phys. Ed.* **1994**, *32*, 205.
(12) Guégan, P.; Macosko, C. W.; Ishizone, T.; Hirao, A.; Nakahama, S. *Macromolecules* **1994**, *27*, 4993.
(13) Frederickson, G. H. *Phys. Rev. Lett.* **1996**, *76*, 3440.
(14) Frederickson, G. H.; Milner, S. T. *Macromolecules* **1996**, *29*, 7386.
(15) O'Shaughnessy, B.; Sawhney, U. *Phys. Rev. Lett.* **1996**, *76*, 3444.
(16) O'Shaughnessy, B.; Sawhney, U. *Macromolecules* **1996**, *29*, 7230.
(17) O'Shaughnessy, B.; Vavylonis, D. *Macromolecules* **1999**, *32*, 1785; *Europhys. Lett.* **1999**, *45*, 638.
(18) Kim, J. K.; Lee, H. *Polymer* **1996**, *37*, 305.
(19) Kim, J. K.; Kim, S.; Park, C. E. *Polymer* **1997**, *38*, 2155.
(20) Kim, S.; Kim, J. K.; Park, C. E. *Polymer* **1997**, *38*, 1809, 2113.
(21) Jeon, H. K.; Kim, J. K. *Polymer* **1998**, *39*, 6227.
(22) Jeon, H. K.; Kim, J. K. *Macromolecules* **1998**, *32*, 9273.
(23) Brosse, J.; Gauthier, J.; Lenain, J. *Makromol. Chem.* **1983**, *184*, 505.
(24) Jeon, H. K.; Kim, J. K. *Korea Polym. J.* **1999**, *7*, 124.
(25) Jeon, H. K.; O, H. T.; Kim, J. K. *Polymer*, in press.
(26) Lee, H. C.; Chang, T.; Harville, S.; Mays, J. W. *Macromolecules* **1998**, *31*, 690.
(27) Lee, H. C.; Lee, W.; Chang, T.; Yoon, J. S.; Frater, D. J.; Mays, J. W. *Macromolecules* **1998**, *31*, 4114.
(28) Kudva, R. A.; Keskkula, H.; Paul, D. R. *Polymer* **1998**, *39*, 2447.
(29) Lepers, J. C.; Favis, B. D.; Tabar, R. J. *J. Polym. Sci., Polym. Phys. Ed.* **1997**, *35*, 2271.
(30) Lepers, J.-C.; Favis, B. D.; Lacroix, C. *J. Polym. Sci., Polym. Phys. Ed.* **1999**, *37*, 939.
(31) Thomas, S.; Groeninckx, G. *Polymer* **1999,** 40, 5799.
(32) Richardson, M. J.; Savill, N. G. *Polymer* **1977**, *18*, 3.
(33) We calculated ρ_{PMMA} at 220 °C using ρ_{PMMA} at T_g and the thermal expansion coefficient, $(1/V)(dV/dT)$ above T_g. $\rho_{PMMA}(T_g)$ is 1.15 g/cm^3, and $(1/V)(dV/dT)$ above T_g is 5.8×10^{-4} K^{-1}.[34]
(34) Brandrup, J., Immergut, E. H., Eds.; *Polymer Handbook*, 3rd ed.; Wiley-Interscience: New York, 1989; p V-77.
(35) Callaghan, T. A.; Paul, D. R. *Macromolecules* **1993**, *26*, 2439.
(36) Schulze, J. S.; Cernohous, J. J.; Hirao, A.; Lodge, T. P.; Macosko, C. W. *Macromolecules* **2000**, *33*, 1191.
(37) Macosko, C. W.; Guégan, P.; Khandpur, A. K.; Nakayama, A.; Marechal, P.; Inoue, T. *Macromolecules* **1996**, *29*, 5590.
(38) Taylor, G. I. *Proc. R. Soc. London* **1932**, *A138*, 41.
(39) Taylor, G. I. *Proc. R. Soc. London* **1934**, *A146*, 501.
(40) Kim, J. K.; Jeong, W. Y.; Son, J. M.; Jeon, H. K. Submitted to *Macromolecules*.
(41) Fortelny, I.; Kovar, J. *Eur. Polym. J.* **1989**, *25*, 317.
(42) Wu, S. *Polym. Sci. Eng.* **1987**, *27*, 335.
(43) Kramer, E. J. *Isr. J. Chem.* **1995**, *35*, 49.
(44) Russell, T. P.; Menelle, A.; Hamilton, W. A.; Smith, G. S.; Satija, S. K.; Majkrzak, C. F. *Macromolecules* **1991**, *24*, 5721.

(45) We used Graessley's equation[46] to estimate D as follows:

$$D = \frac{G_N^0}{135}\left(\frac{\rho RT}{G_N^0}\right)^2\left(\frac{\langle r^2\rangle}{M}\right)\left(\frac{M_c}{M^2}\right)\frac{1}{\eta_0(M_c)}$$

where G_N^0 is the shear modulus, 2×10^5 Pa, $\langle r^2\rangle^{1/2}$ is the end-to-end distance, 27 nm, $M_c = 31\,000$, $\rho = 0.96$ g/cm^3, and $\eta_0(M_c)$ at 220 °C = 5.0 Pa·s.[47]

(46) Graessley, W. W. *J. Polym. Sci., Polym. Phys. Ed.* **1980**, *18*, 27.

(47) We calculated $\eta_0(M_c)$ at 220 °C from the value (120 Pa·s) of $\eta_0(M_c)$ at 174 °C[48] using WLF equation with the constants $c_1 = -13.7$ and $c_2 = 50$.[49]

(48) Green, P. D. Ph.D. Thesis, Cornell University, 1985.

(49) Ferry, J. D. *Viscoelastic Properties of Polymers*; John Wiley & Sons: New York, 1980.

(50) We assumed that k between PS-mCOOH and PMMA-GMA with many epoxy groups is the same as that between PS-mCOOH and epoxy terminal PMMA (PMMA-E) with only one epoxy group. In ref 12, k at 180 °C and the activation energy, E_a, are 0.05 kg mol^{-1} s^{-1} and 84 kJ/mol, respectively. Using E_a, k at 220 °C is 6 times larger than that at 180 °C.

(51) Jiao, PHD Dissertation, Cornell University, 1997.

(52) Dedecker, K.; Groeninckx, G. *Macromolecules* **1999**, *32*, 2479.

(53) Koriyama, H.; Oyama, H.; Ougizawa, T.; Inoue, T.; Weber, M.; Koch, E. *Polymer* **1999**, *40*, 6381.

(54) Xanthos, M., Ed.; *Reactive Extrusion*: *Principles and Practice*: Hanser: New York, 1992.

MA000842I